Available online at www.sciencedirect.com

ScienceDirect

Procedia Engineering 213 (2018) 313–322

Procedia Engineering

www.elsevier.com/locate/procedia

7th International Conference on Fatigue Design, Fatigue Design 2017, 29-30 November 2017, Senlis, France

The Dissipated Heat Energy as a Fatigue Damage Index For Experimental Fatigue Life Estimations

G. Meneghetti*, M. Ricotta

University of Padova, Department of Industrial Engineering, via Venezia, 1, 35131 Padova, Italy

Abstract

In the last decade, the heat energy dissipated in a unit volume of material per cycle (the Q parameter) has been adopted by the authors as a fatigue damage indicator of metallic materials. The advantage of using such a parameter is that it can be readily and in-situ measured at a point or a component undergoing fatigue solicitations. Geometrical, mean stress and variable amplitude (limited to two stress-level tests) effects have been successfully analysed by using the Q parameter. Concerning geometrical effects, approximately 160 experimental results generated from constant amplitude, completely reversed, stress- or strain-controlled fatigue tests on plain or notched hot rolled as well as cold drawn stainless steel specimens have been rationalised. Afterwards, the heat-energy based approach was extended to include the mean stress effect, by using a thermodynamic fatigue damage variable that combines two parameters, i.e. Q and the thermoelastic temperature achieved by the material at the maximum stress of the load cycle. Finally, Q was used to rationalise two stress-level fatigue test results, by using the Q-based fatigue curve combined with Miner's rule. In this paper, the theoretical background and the application of the energy-based approach are reviewed in order to analyse all previously mentioned effects, focusing mainly on the mean stress and the variable amplitude, two stress-level effects.

Peer-review under responsibility of the scientific committee of the 7th International Conference on Fatigue Design.

Keywords: Type your keywords here, separated by semicolons ;

* Giovanni Meneghetti. Tel.: 0039 049 827 6758; fax: 0039 827 6785.
E-mail address: giovanni.meneghetti@unipd.it

1877-7058
Peer-review under responsibility of the scientific committee of the 7th International Conference on Fatigue Design.
10.1016/j.proeng.2018.02.032

1. Introduction

Fatigue of metallic materials is an irreversible process, accompanied by microstructural changes, localised plastic strains and energy dissipation, which requires a certain amount of mechanical energy in a unit volume of material, W. Only part of this energy is accumulated in the form of internal energy, E_p, which is responsible for fatigue damage accumulation and final fracture. The remaining part is dissipated as heat [1], thus translating into some temperature increase during fatigue testing. The thermal energy dissipated in a unit volume of material per cycle (the Q parameter) has been adopted as a fatigue damage indicator during fatigue tests of stainless steel specimens and a relatively simple experimental technique has also been proposed to estimate Q from in-situ measurements of the temperature at the surface of a specimen or a component [2]. Similar to W, Q is thought of as a material property, i.e. it is independent, within certain limits, of the thermal, mechanical and geometrical boundary conditions of the laboratory fatigue tests [3]. Then, the specific heat loss per cycle Q at a given point of a component (similar to the plastic hysteresis energy) depends only on the applied load cycle, defined by amplitude, mean value and stress state.

The Q parameter was initially adopted to rationalise geometrical effects in fatigue of metallic [3-7] as well as composite materials [8]. Afterwards, the heat-energy based approach was extended to include the mean stress effect [9], as well as to rationalise two stress level fatigue test results of steel materials [10]. Finally, in order to extend the heat energy method to severely notched or cracked materials, the specific heat energy per cycle was averaged in a control volume of material, Q*, located at the notch or crack tip [11].

In this paper, the theoretical basis of the Q-based approach is first reviewed along with its applications in notch fatigue with zero mean stress. Subsequently, its more recent extension to include the mean stress as well as the two stress-level effects in fatigue are presented.

2. Theoretical background at constant amplitude, zero-mean stress loading

The first law of thermodynamics applied over one loading cycle to a unit volume of material, V, can be written as [2]

$$\int_V W \cdot dV = \int_V (Q + \Delta U) \cdot dV \tag{1}$$

W being the input mechanical energy (the area within the hysteresis cycle), Q the dissipated thermal energy and ΔU the variation of internal energy. Eq 1 can be written considering the mean power exchanged over one loading cycle:

$$\int_V \left(\oint \sigma_{ij} \cdot d\varepsilon_{ij} \right) \cdot f_L \cdot dV = \int_V H \cdot dV + \int_V \left(\rho \cdot c \cdot \frac{\partial T_m(t)}{\partial t} + \dot{E}_p \right) \cdot dV \tag{2}$$

where f_L is the load test frequency, $H=Q \cdot f_L$ is the thermal power dissipated by conduction, convection and radiation, ρ the material density, c the specific heat and $\dot{E}_p$ the rate of accumulation of damaging energy in a unit volume of material. Since Eq. (2) considers the rate of energy contributions averaged over one cycle, the thermoelastic effect does not produce a net energy dissipation or absorption over one loading cycle, consisting of a reversible exchange between mechanical and thermal energy. Therefore, the mean temperature evolution $T_m(t)$ (see Fig. 1) appears in the right side of Eq. 2. When temperature stabilises, the first derivative of $T_m(t)$ becomes null, therefore Eq.2 simplifies to:

$$\int_V \left(\oint \sigma_{ij} \cdot d\varepsilon_{ij} \right) \cdot f_L \cdot dV = \int_V H \cdot dV + \int_V \dot{E}_p \cdot dV \tag{3}$$

If referred to a point on the specimen's surface, Eq. 3 becomes

$$W \cdot f_L = H + \dot{E}_p \tag{4}$$

Suppose now to stop suddenly the fatigue test at t=t* (Fig. 1): then just after t* (i.e. at t=t*+) the mechanical input power $W \cdot f_L$ as well as the rate of accumulation of fatigue damage $\dot{E}_p$ will vanish. By writing again the energy balance equation (2), one can obtain:

$$\rho \cdot c \cdot \left. \frac{\partial T(t)}{\partial t} \right|_{t=(t^*)^+} = -H \tag{5}$$

It is worth noting that the thermal power H dissipated to the surroundings just before and just after t* is the same in Eq. (4) and in Eq. (5), respectively, because the temperature field is continuous through t*. Finally, the thermal energy released in a unit volume of material per cycle can be calculated by simply accounting for the load test frequency, f_L:

$$Q = \frac{H}{f_L} = -\frac{\rho \cdot c \cdot \left. \frac{\partial T(t)}{\partial t} \right|_{t=(t^*)^+}}{f_L} \tag{6}$$

Eq. (6) enables one to measure readily and in-situ the specific heat loss Q at any point of a specimen or a component undergoing fatigue loadings. In all the experimental tests carried out by the authors, Q was found quite constant during a single fatigue test.

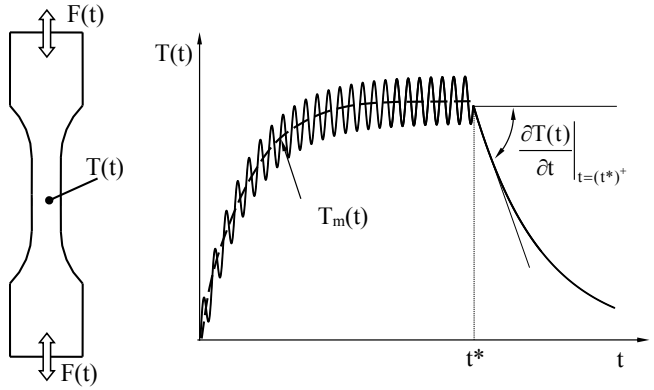

Fig. 1. Evaluation of the cooling gradient Eq. (6) during a fatigue test.

3. Analysis of geometrical effects in constant amplitude, fully reversed fatigue loading

As stated above, the Q parameter was initially adopted to rationalise in a single scatter band approximately 160 experimental results generated from constant amplitude, completely reversed, stress- or strain-controlled fatigue tests on plain or notched hot rolled stainless steel specimens, having notch radius r_n=3, 5, 8 mm [3,4] and r_n=0.5, 1 and 3 mm [5-7], as well as from cold drawn un-notched bars of the same steel, under fully-reversed axial or torsional fatigue loadings [12]. Fig. 2a shows the axial and torsional fatigue test results in terms of net-section stress amplitude σ_{an} or τ_a, respectively, the mean curve and the 10%-90% survival probability scatter band. The same fatigue data reanalysed in terms of Q are shown in Fig. 2b. In particular, the 10%–90% scatter band shown in the

figure was fitted only on the fatigue data published in [3]. However, Fig 2b shows that the same scatter band can interpret all fatigue data.

As it can be shown in the next Fig. 4 and according to [13], the Q parameter is influenced by the presence of a mean stress different from zero and then it can not correlate fatigue data obtained in different mean stress condition. Therefore, in [9] the Q energy-based was extended to overcome this drawback, as discussed in the next section.

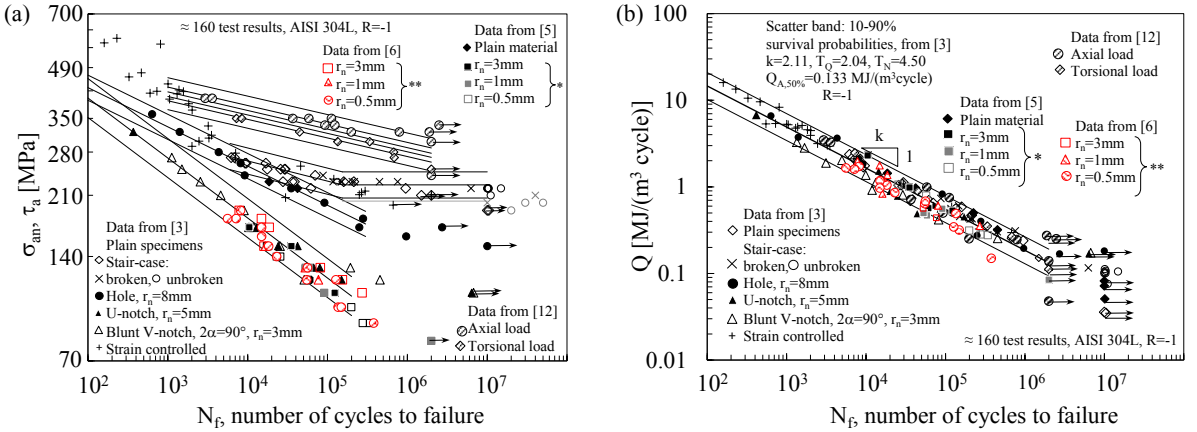

Fig. 2. Fatigue test results reanalysed in term of net-section stress amplitude (a) and of specific heat energy (b). The scatter band was calibrated only on data published in [3] (notch opening angle *=90°, **=135°).

4. Analysis of the mean stress influence in constant amplitude fatigue

The presence of a mean stress different from zero was included in the energy-based approach [9], inspired by stress as well as strain-based approaches available in literature. Some of these are based on the combination of two different mechanical parameters: the amplitude (or range) of the driving force and its level, by means of its maximum level. As an example, dealing with Fracture Mechanics field, Walker [14] and more recently Vasudevan et al [15], Kujawski [16,17] and Stoychev and Kujawski [18] suggested to use an equivalent stress intensity factor to correlate crack growth data obtained from fatigue tests carried out at different load ratios, according to Eq. 7

$$\Delta K_{eqv} = \Delta K^{(1-\alpha)} \cdot K_{max}^{\alpha} \tag{7}$$

where ΔK, K_{max} are the range and the maximum value of the stress intensity factor, respectively, and α is a best fitting parameter to be determined by fitting the experimental data. Regarding strain-based approaches, Smith, Watson and Topper [19] proposed the SWT parameter to include the mean stress effect in the strain-life approach to notch fatigue

$$SWT = \sqrt{\sigma_{max} \cdot E \cdot \varepsilon_a} \tag{8}$$

being σ_{max}, E and ε_a the maximum stress, the material elastic modulus and the elasto-plastic strain amplitude, respectively. In [9], the amplitude and the maximum level involved in Eq (7) and Eq (8) were considered from a thermodynamic point of view, i.e it was assumed that the fatigue strength is correlated to a thermodynamic exchange variable (the amplitude of the driving force) as well as to a state variable, corresponding to its level. Accordingly, the Q parameter was identified as the exchange variable, whereas the thermoelastic temperature T_{the} was assumed as the state variable. More precisely, the thermoelastic temperature T_{the} has been assumed equal to the temperature that would be reached by the material when loaded at the maximum stress level of the fatigue cycle, σ_{max}, in an adiabatic process. Therefore, the following fatigue life equation was proposed to rationalise the mean stress influence on axial fatigue:

$$\left(Q \cdot \left(\frac{|T_{the}|}{T_0} \right)^h \right)^m \cdot N_f = \left(\overline{Q} \right)^m \cdot N_f = \text{const} \tag{9}$$

where h and m are material constants that can be calculated fitting the experimental data and T_0 is the material temperature at the beginning of the adiabatic loading process. Regarding T_{the}, it can be evaluated experimentally by loading the material in its elastic field and then by measuring the corresponding temperature variation or it can be easily calculated from Eq. 10, which relates T_{the} to the maximum applied stress:

$$\frac{T_{the}}{T_0} = -\left(\frac{\alpha}{\rho \cdot c} \right) \cdot \sigma_{max} = -K_m \cdot \sigma_{max} \tag{10}$$

where α is the material thermal expansion coefficient. It is worth noting that in the case of cold drawn AISI 304L stainless steel as well as quenched and tempered C45 steel, adiabatic conditions can be easily achieved in standards laboratory tests [9] and the following thermoelastic constants were measured $K_m = 3.75 \cdot 10^{-12}$ Pa^{-1} and $2.75 \cdot 10^{-12}$ Pa^{-1}, respectively.

The proposed approach was validated by considering two different materials, namely 25-mm-diameter bars made of cold drawn AISI 304L or hot rolled quenched and tempered (Q&T) C45 steel, having the mechanical properties and the chemical composition listed in Table 1. For the details of specimen geometry as well as experimental tests, the reader is referred to [9]. In this paper, it is mentioned that constant-amplitude stress controlled fatigue tests were carried out by imposing four different load ratios R (R=-1.5 (R=-2 for Q&T C45), R=-1, R=0.1 and R=0.5). During each fatigue test, at least 5 stops were performed in order to measure the cooling gradient and to monitor the Q parameter evolution, according to Eq. (6). The stainless steel had a material density ρ and the specific heat c equal to 7940 kg/m^3 and 507 J/(kg K), respectively [20]. For the Q&T C45 steel, ρ was assumed equal to 7850 kg/m^3 and c equal to 486 J/(kg K) [21]. The specimen's temperature was measured by using copper-constantan thermocouple (Type T) wires having diameter 0.127 mm, which were fixed at the specimen's centre by means of a silver-loaded conductive epoxy glue. Temperature signals generated by the thermocouples were acquired by means of a data logger Agilent Technologies HP 34970A operating at a maximum sample frequency, f_{acq}, equal to 22 Hz.

Table 1. Cold drawn AISI 304L stainless steel and quenched and tempered C45 material properties.

Material	E [MPa]	R_{p02}, R_y [MPa]	R_m [MPa]	A [%]	C [wt%]	Si [wt%]	Mn [wt%]	Cr [wt%]	Mo [wt%]	Ni [wt%]	Cu [wt%]
AISI 304L	192200	468	691	43	0.013	0.58	1.81	18.00	0.44	8.00	0.55
Q&T C45	205500	580	771	25	0.46	0.24	0.63	0.15	0.02	0.08	0.10

Fatigue tests results are shown in Fig. 3 in terms of the engineering stress amplitude σ_a for AISI 304L and Q&T C45 specimens. The figure reports the mean curves, the 10%-90% survival probability scatter bands, the inverse slope k, the reference fatigue strength $\sigma_{A,50\%}$ evaluated at N_A= 2 million cycles with a survival probability equal to 50%, and the stress- as well as the life-based scatter index T_σ ($T_\sigma = \sigma_{A,10\%}/\sigma_{A,90\%}$) and $T_{N,\sigma}$, respectively. The experimental data were statistically analysed under the hypothesis of log-normal distribution of the number of cycles to failure with a 95% confidence level. As it can be expected, both materials are sensitive to the stress ratio.

As stated above, during a single fatigue test several stops were made to monitor he evolution of Q parameter. It was observed that in the case of stainless steel specimens, Q values ranged between 0.01 and 5 MJ/(m^3·cycle), that means a factor of 500, in spite of a variation of σ_a from 155 to 400 MPa, i.e a factor of only 2.58. Regarding Q&T C45 specimens, Q varied from 10^{-3} to 1.2 MJ/(m^3 cycle) (i.e. a factor of 1200), in spite of a variation of the stress amplitude from 150 to 400 MPa, that means a factor of only 2.67 [9].

The fatigue tests results plotted in Fig. 3 were reanalysed in terms of the Q parameter measured at the 50% of the fatigue life or 2 million cycles in the case of run-out specimens. Results are shown in Fig. 4a and 4b for AISI 304L

and Q&T C45 steel, respectively. $Q^k \cdot N_f$ =const is the expression of the mean and the 10% - 90% survival probability curves fitting the experimental results with a confidence level of 95%. It can be observed that $Q_{A,50\%}$ value of the AISI 304L is always higher than that of Q&T C45 steel for the same stress ratio, a factor ranging from 2.6 (R=0.5) to 3.7 (R=0.1) being valid. Finally, Fig. 4a and 4b show that the specific heat loss Q can not rationalise the fatigue data generated at different load ratios. Therefore, Eq. 9 was adopted to correlate the fatigue data [9].

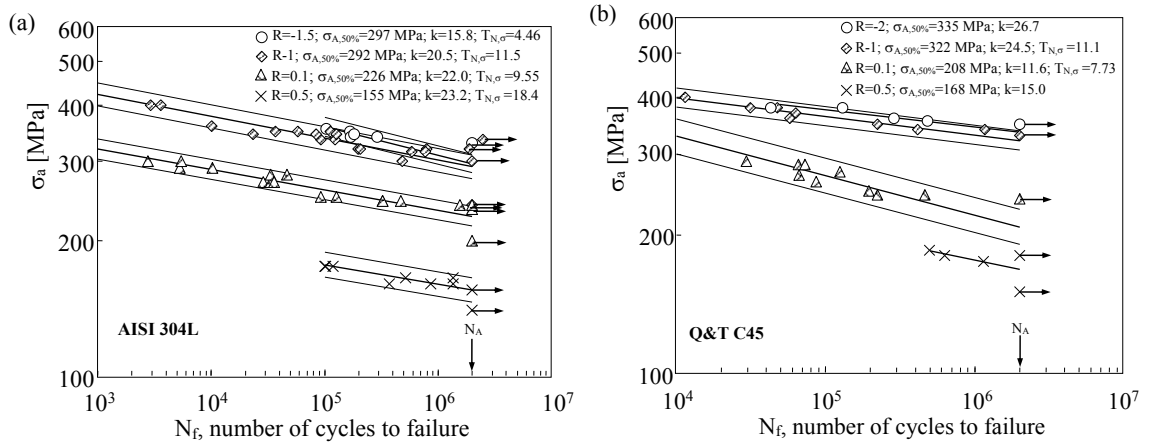

Fig. 3. Fatigue test results for the (a) AISI 304 L and (b) Q&T C45 steel specimens in terms of stress amplitude for different load ratios. Scatter bands are defined for 10% and 90% survival probabilities.

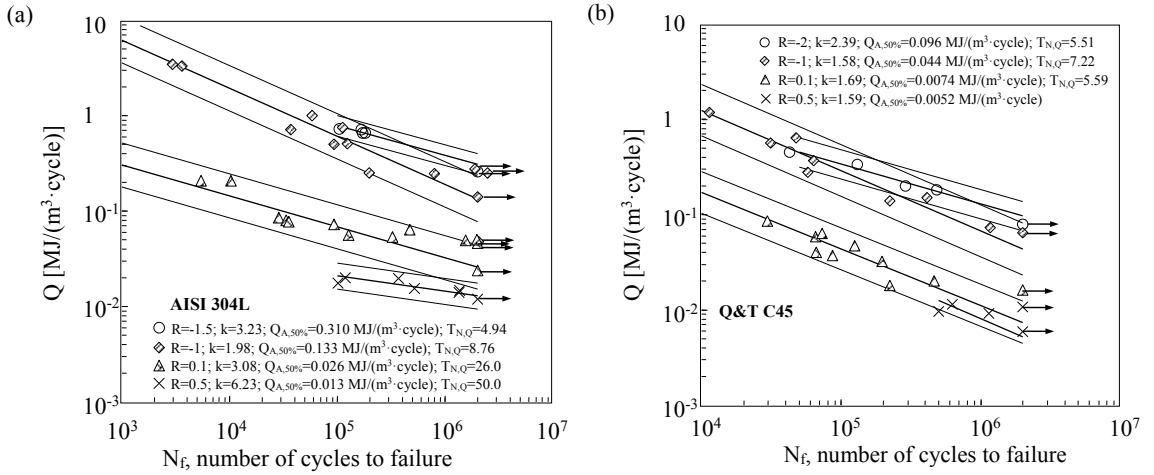

Fig. 4. Fatigue data analysed in terms of specific heat loss. Scatter bands are defined for 10% and 90% survival probabilities.

Once K_m is measured or calculated, the thermoelastic temperature relevant to each specimen was calculated according to Eq. 10. Then having Q, $|T_{the}|/T_0$ and the number of cycles to failure N_f for each specimen, the material parameters h of Eq. 9 was calculated as follows. The experimental results were plotted in a Q versus $|T_{the}|/T_0$ diagram, using N_f as a parameter, according to Fig.5. By considering all available data and independently of the load ratio R, the fatigue test results were divided in different groups, according to the number of cycles to failure. Dashed regression lines in the log-log diagram of Fig. 5 were calculated for each group. Considering the limited variation of h, it can be concluded that $\overline{Q} = Q \cdot (T_{the}/T_0)^h$ can be considered an efficient fatigue damage parameter, being h a material parameter, which describes the sensitivity to mean stresses. The lower h is, the weaker the material sensitivity to the mean stress. Fig. 5 shows a resulting value of h=4.03 for AISI 304L and 2.76 for Q&T C45.

Fig. 6 shows that all the fatigue data reanalysed in terms of $\overline{Q}$, according to Eq.(9), fall in a single scatter band, independently of the load ratio. The hypothesis of the log-normal distribution of the number of cycles to failure with

95% confidence level was adopted. Fig. 6a and 6b report the mean line, the 10% - 90% survival probability curves, the inverse slope m, and the temperature-corrected energy- $T_{\overline{Q}}$ and the life- $T_{N,\overline{Q}}$ scatter indexes, for AISI 304L and Q&T C45, respectively. By comparing the $T_{N,\overline{Q}}$ in Fig. 6 with the $T_{N,\sigma}$ and $T_{N,Q}$ indexes reported in previous Figs. 3 and 4, it can be observed that new $\overline{Q}$ parameter is able to rationalise all fatigue data into a single scatter band valid for each material, having a constant slope from 10^3 (10^4 for Q&T C45 steel) to $2 \cdot 10^6$ cycles, despite the different load ratios involved.

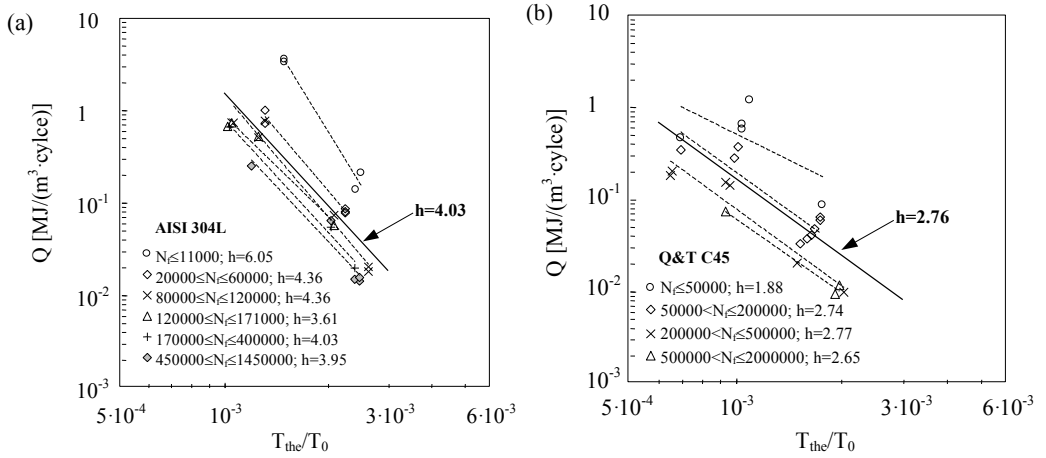

Fig. 5. Evaluation of the material parameter h for (a) AISI 304L and (b) Q&T C45

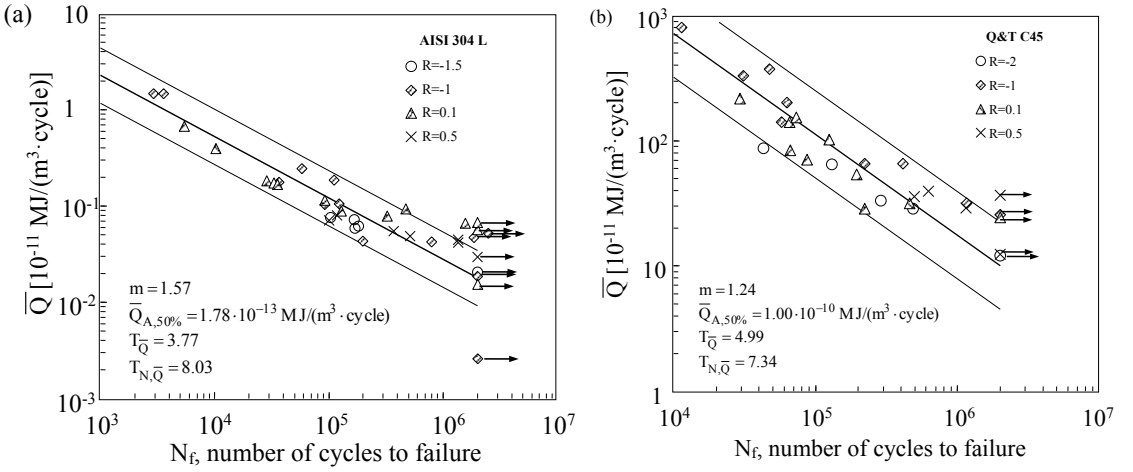

Fig. 6. Fatigue data of Fig. 4 analyzed in terms of $\overline{Q}$. Scatter bands are defined for 10 and 90% survival probabilities.

5. Analysis of two stress-level loading

The Q parameter was successfully adopted to rationalise fatigue data obtained by carrying out two stress-level fatigue tests on plain specimens, machined from 6-mm-thick hot rolled AISI 304L stainless steel sheets, having the material properties listed in Table 2 [10]. First, constant amplitude fatigue tests were carried out to evaluate the material stress-life curve and the fatigue limit, $\sigma_{A,-1}$, by means of a stair case procedure at 10 million cycles. Then two-stage fatigue tests were conducted, the second stress level being applied up to the specimen's failure or to 10 million cycles (run-out specimen). Both High-Low (HL) and Low-High (LH) load sequences were adopted. In [10], in order to measure the Q parameter by Eq. 6, surface temperature was monitored by using a THERMOVISION

A40 infrared camera with ThermaCAM™ Research 2.8 SR-1 software for image processing. For additional details, the reader is referred to [10].

Results of constant amplitude fatigue tests reanalysed in terms of stress-amplitude as well as Q parameter are shown in Fig. 7a and 7b, respectively, with the inverse slope of the curves k, the stress-based T_σ as well as the life-based scatter index $T_{N,\sigma}$. One can observe that the life-based scatter index relevant to the Q-based scatter band $T_{N,Q}$ is lower than $T_{N,\sigma}$, since it was experimentally observed that for the same applied nominal stress amplitude the lower the number of cycles to failure, the higher the Q values, as it can be seen by considering the data marked by the "#" symbol.

Concerning the two-stage fatigue tests, four different load sequences were analysed for both HL and LH fatigue tests and different fractions of fatigue life n/N_f were spent in the first stage.

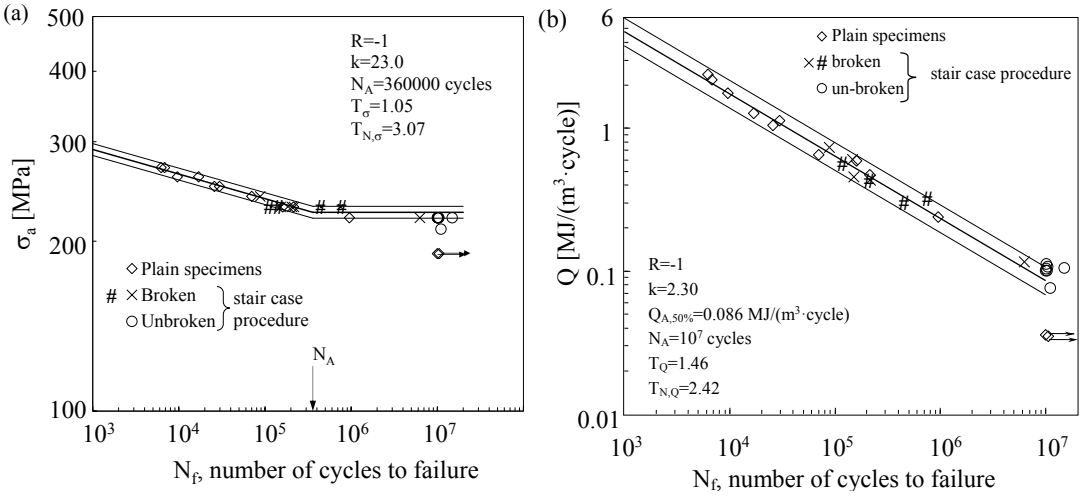

Fig. 7. Constant amplitude fatigue test results reanalysed in terms of (a) stress amplitude and (b) Q parameter. Scatter bands are defined for 10% and 90% survival probabilities.

Table 2. Hot rolled AISI 304L stainless steel material properties.

E [MPa]	R_{p02} [MPa]	R_m [MPa]	A [%]	C [wt%]	Si [wt%]	Mn [wt%]	Cr [wt%]	Mo [wt%]	Ni [wt%]	Cu [wt%]
194700	315	700	66	0.020	0.34	1.67	18.00	0.44	8.08	0.29

Damage D induced during the two-stage fatigue tests was evaluated according to Miner's rule [22]:

$$D = \sum_{i=1}^{2} \frac{n_i}{N_i} = \frac{n_L}{N_{f,L}} + \frac{n_H}{N_{f,H}} \tag{11}$$

where n_L and n_H are the number of cycles expended at low and high stress amplitude, respectively, while $N_{f,L}$ and $N_{f,H}$ are the relevant number of cycles to failure, that can be assessed on the basis of the stress- (see Fig. 7a) or Q-based curves (see Fig. 7b). Results are reported in Fig. 8a and 8b, respectively. Figure 8a compares the experimental results with Miner's hypothesis (D=1) based on the 50% survival probability S-N curve: the horizontal and the vertical axis represent the life fraction spent at low and high stress level, respectively. Better agreement with Miner's rule exists for HL than for LH load sequences [10]. Moreover, when two load level fatigue test results are re-analysed in Fig. 8b by using the energy parameter Q as damage variable, much better agreement with Miner's rule is obtained. In the authors' opinion, this result can be interpreted as a better capability of the Q parameter to account

for the actual material cyclic evolution with respect to the applied stress amplitude. In [10], this effectiveness of Q was justified recalling that the Miner's rule was originally proposed on the basis of energy considerations [22]. In fact one can suppose that, in constant amplitude fatigue tests, E_p is a function of σ_a, $E_p(\sigma_a)$, and it may be assumed constant with loading cycles, at least as a first approximation. However, E_p depends also on the previous stress amplitude in two-stage fatigue tests. Conversely, the specific energy stored in a unit volume of material at fatigue fracture, $E_{p,f,}$ is a material constant at fracture and it is independent of the applied stress amplitude. In a two-stage fatigue test with first stress amplitude equal to σ_{a1} and second stress amplitude equal to σ_{a2} the energy stored at fracture $E_{p,f}$ can be expressed as:

$$E_{p,f} = E_p(\sigma_{a1}) \cdot n_1 + E_p(\sigma_{a2}) \cdot n_2 \tag{12}$$

Being a material property, $E_{p,f}$ can be expressed by considering the E_p values, E_{p1} and E_{p2}, relevant to constant amplitude fatigue tests, where we suppose that the damage accumulation rate is equal to that observed in the two-stage test, respectively, i.e. $E_{p1}=E_p(\sigma_{a1})$ and $E_{p2}=E_p(\sigma_{a2})$. Therefore, being $E_{p,f} = E_{p1} \cdot N_{f,1} = E_{p2} \cdot N_{f,2}$, we have:

$$\frac{E_p(\sigma_{a1}) \cdot n_1}{E_{p1} \cdot N_{f,1}} + \frac{E_p(\sigma_{a2}) \cdot n_2}{E_{p2} \cdot N_{f,2}} = 1 \tag{13}$$

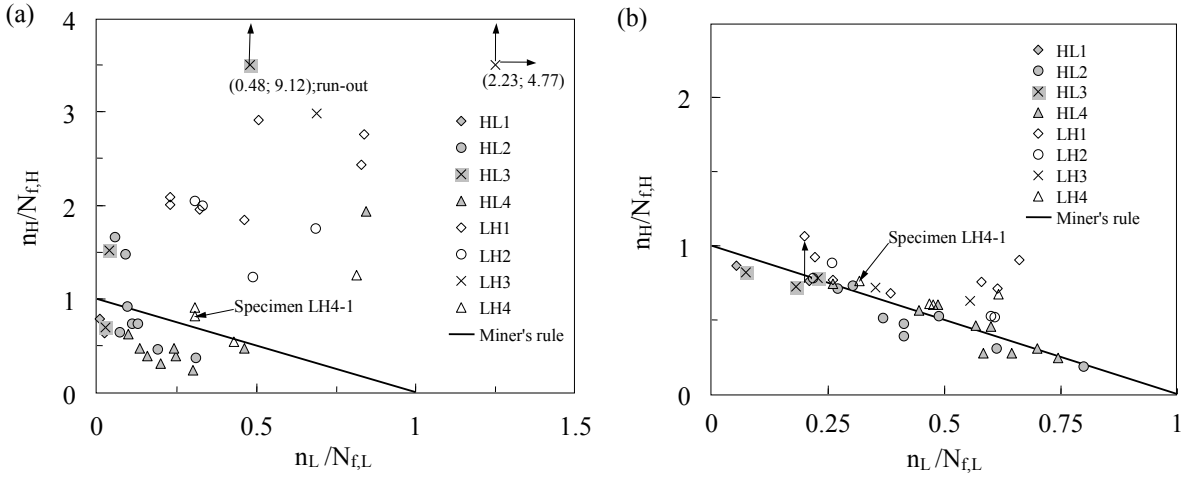

Fig. 8. (a) Stress- and (b) energy-based two – stage fatigue test results.

It should be noted that σ_{a1} is the applied constant stress amplitude in order to have E_{p1}; however, due to the effects of the previous load history on cyclic material behaviour, the stress amplitude to be applied to have E_{p2} is not σ_{a2}. Eq. (12) is the Miner's rule and it says that the number of cycles N_f must be that relevant to the damage accumulation rate actually existing during the considered load stage. For the same applied stress amplitude, different damage accumulation rate might exist due to different evolutions of the material cyclic behaviour or to previous load history effects. Differently from the applied stress, the specific heat loss Q proved to better take into account the actual damage accumulation rate existing during the considered load stage.

6. Conclusions

This paper presented a review of the theoretical and experimental activity carried out by the authors in the last decade to conceive and apply a new energy-based fatigue damage indicator, which consists in the heat energy dissipated by a unit volume of material per cycle, i.e. the so-called Q parameter. After recalling the theoretical frame and the experimental technique developed to measure Q, the paper is focused on the recent extensions made by the

authors to account for the mean stress effect and variable amplitude, two stress-level fatigue test results. In the former case, the Q-based approach was developed by using a thermodynamic fatigue damage variable, $\underline{Q}$, that combines two parameters, i.e. Q and the thermoelastic temperature achieved by the material at the maximum stress of the load cycle. The $\underline{Q}$ parameter allowed the fatigue data to be rationalised in a single scatter band, valid for each analysed material, namely a cold drawn AISI 304 L and a hot rolled quenched and tempered C45 steel subjected to different load ratios. Concerning two stress-level fatigue tests, constant amplitude and two-stage loading fatigue tests were performed on an AISI 304 L stainless steel material. Results were presented both in terms of applied nominal stress amplitude and in terms of the Q parameter. Two-stage loading results were compared with estimations based on Miner rule. It was found that when using the energy parameter as damage variable better correlation was obtained. The reason for that was attributed to the nature of the energy parameter which measures the actual material response to the external applied stress.

Acknowledgements

This work was carried out as a part of the Italian Research Program PRIN 2009Z55NWC of the Ministry of University and Scientific Research. The Authors would like to express their gratitude for financial support.

References

[1] F. Ellyin, Fatigue damage, crack growth and life prediction. Chapman & Hall, London, 1997
[2] G. Meneghetti, Analysis of the fatigue strength of a stainless steel based on the energy dissipation, Int J Fatigue, 29 (2007), 81-94
[3] G. Meneghetti, M. Ricotta, B. Atzori, A synthesis of the push-pull fatigue behaviour of plain and notched stainless steel specimens by using the specific heat loss, Fatigue Fract Engng Mater Struct, 36 (2013), 1306-1322
[4] G. Meneghetti, M. Ricotta, The use of the specific heat loss to analyse the low- and high cycle fatigue behaviour of plain and notched specimens made of a stainless steel, Eng Fract Mech 81 (2012), 2-16.
[5] G. Meneghetti, M. Ricotta, B. Atzori, The heat energy dissipated in a control volume to correlate the fatigue strength of bluntly and severely notched stainless steel specimens, Procedia Structural Integrity 2 (2016), 2076–83.
[6] D. Rigon, M. Ricotta, G. Meneghetti, The use of the heat energy loss to correlate the fatigue strength of severely notched stainless steel specimens. Proceedings of International Symposium on Notch Fracture ISNF, Santander, Spain, 29-31 March, 2017
[7] G. Meneghetti, M. Ricotta, D. Rigon, The heat energy dissipated in a control volume to correlate the fatigue strength of severely notched and cracked stainless steel specimens, Proceedings of International Fatigue Conference, Cambridge, UK, 3-5 July 2017.
[8] G. Meneghetti, M. Quaresimin, Fatigue strength assessment of a short fiber-reinforced composite based on the specific heat dissipation, Comp B, 42 (2011) 217-225
[9] G. Meneghetti, M. Ricotta, B. Atzori, A two-parameter, heat energy-based approach to analyse the mean stress influence on axial fatigue behaviour of plain steel specimens. Int J Fatigue, 82 (2016) 60-70
[10] G. Meneghetti, M. Ricotta, B. Atzori, Experimental evaluation of fatigue damage in two-stage loading tests based on the energy dissipation. P I Mech Eng C-J Mec, 229 (2015), 1280-1291.
[11] G. Meneghetti, M. Ricotta, Evaluating the heat energy dissipated in a small volume surrounding the tip of a fatigue crack. Int J Fatigue, 92 (2016), 605-615.
[12] G. Meneghetti, M. Ricotta, L. Negrisolo, B. Atzori, A synthesis of the fatigue behavior of stainless steel bars under fully reversed axial or torsion loading by using the specific heat loss, Key Eng Mat, 577–578 (2013), 453–6.
[13] C. Mareau, V. Favier, B. Weber, A. Galtier. Influence of the free surface and the mean stress on the heat dissipation in steels under cyclic loading. Int J Fatigue, 31 (2009), 1407–1412.
[14] K. Walker. The effect of stress ratio during crack propagation and fatigue for 2024-T3 and 7075-T6 aluminum. ASTM STP 462, 1970, 1-14.
[15] AK. Vasudevan, K. Sadananda, G. Glinka. Critical parameters for fatigue damage. Int J Fatigue, 23S (2001), S39-S53.
[16] D. Kujawski. A new $(\Delta K^{+} \cdot K_{max})^{0.5}$ driving force parameter for crack growth in aluminum alloys. Int J Fatigue, 23 (2001), 733-740.
[17] D. Kujawski. A fatigue crack driving force parameter with load ratio effects. Int. J. Fatigue, 23 (2001), S239-S246.
[18] S. Stoychev, D. Kujawski. Analysis of crack propagation using ΔK and K_{max}. Int. J. Fatigue, 27 (2005), 1425-1431.
[19] KN. Smith, P. Watson, TH. Topper. A stress-strain function for the fatigue of metals. J Mater, 5 (1970), 767-778.
[20] B. Atzori, G. Meneghetti, M. Ricotta. Analysis of the fatigue strength under two load levels of a stainless steel based on energy dissipation. The European Physical Journal EPJ Web of Conferences volume 6-2010.
[21] ASTM, Metal handbook - 9th ed., vol. 3; 1990.
[22] MA. Miner, Cumulative damage in fatigue. In: ASME conference of the Aviation Division, Los Angeles, USA, June 16-17 1945.